

# Supporting information for: Energy transfer in ssDNA-templated stacks of naphthalene chromophores

Amy L. Stevens,<sup>†</sup> Pim G. A. Janssen,<sup>‡</sup> Amparo Ruiz-Carretero,<sup>‡</sup> Mathieu Surin,<sup>¶</sup>  
Albertus P. H. J. Schenning,<sup>‡</sup> and Laura M. Herz<sup>\*,†</sup>

*Clarendon Laboratory, Parks Road, Oxford OX1 3PU, United Kingdom, Laboratory for  
Macromolecular and Organic Chemistry, Group Theoretical and Polymer Physics, and Institute  
for Complex Molecular Systems, Eindhoven University of Technology, P.O. Box 513, 5600 MB  
Eindhoven, The Netherlands, and Laboratory for Chemistry of Novel Materials, University of  
Mons — UMONS, 20 Place du Parc B-7000 Mons*

E-mail: l.herz1@physics.ox.ac.uk

## Synthesis and characterisation

### General methods

<sup>1</sup>H NMR and <sup>13</sup>C NMR were recorded at room temperature on a Varian 300 or Varian Mercury 400. Chemical shifts are given in ppm ( $\delta$ ) relative to tetramethylsilane. Abbreviations used are s = singlet, d = doublet, dd = double doublet, t = triplet and m = multiplet. Infrared (IR) spectra

---

\*To whom correspondence should be addressed

<sup>†</sup>Clarendon Laboratory, Oxford, UK

<sup>‡</sup>Laboratory for Macromolecular and Organic Chemistry, Eindhoven University of Technology

<sup>¶</sup>Laboratory for Chemistry of Novel Materials, University of Mons — UMONS

were run on a Perkin Elmer 1600 FT-IR spectrometer. MALDI-TOF MS spectra were measured on a Perspective DE Voyager spectrometer utilizing an  $\alpha$ -cyano-4-hydroxycinnamic acid matrix. CD and UV-vis were recorded on a JASCO 815 equipped with a Peltier temperature controller, PFD-425S.

## Sample preparation

All NP-containing samples were prepared by adding a *Tn* to molecularly-dissolved NP in MilliQ water at the concentrations stated in the main manuscript.

## Materials

Trityl tetraethylene glycol *p*-tosyl diether, **2**,<sup>[1]</sup> and tetraethylene glycol mono(*tert*-butyldiphenylsilyl) ether, **5**,<sup>[2]</sup> were synthesized according to literature procedures. The ssDNA was supplied HPLC purified and freeze-dried by MWG Biotech AG. All solvents, purchased from Acros Chimica or Sigma-Aldrich-Fluka, were of p.a. quality. Dry DMF and THF were obtained by distillation. Deuterated solvents were from Cambridge Isotope Laboratories. All other chemicals were commercially available and were used without purification.

## Synthesis

The diaminopurine-naphthalene guest molecule (**G**) was synthesized via a convergent route (Figure Figure 1). Commercial 2,6-diaminopurine was subjected to a selective alkylation reaction with the trityl-protected tetraethylene glycol *p*-tosyl ether **2**, via a reported procedure.<sup>[3]</sup> Subsequent bromination of **3** in the presence of *N*-bromosuccinimide afforded diaminopurine **4** in good yields. On the other hand, the ethynyl-2-naphthalene tetraethylene glycol derivative (**10**) was obtained via a Sonogashira coupling reaction between 6-bromo-2-naphthol (**7**) and triisopropylsilylethyne (TIPSE), followed by an alkylation reaction with the *tert*-butyldiphenylsilyl-protected tetraethylene glycol *p*-tosyl ether **6**, and subsequent deprotection using tetra-*n*-butylammonium fluoride

(TBAF). The cross-coupling reaction between the 8-bromopurine derivative **4** and the ethynyl-naphthalene **10** was carried out under copper-free Sonogashira conditions<sup>[4]</sup> yielding precursor **11**. Deprotection of **11** in the presence of trifluoroacetic acid (TFA) affords **G**.

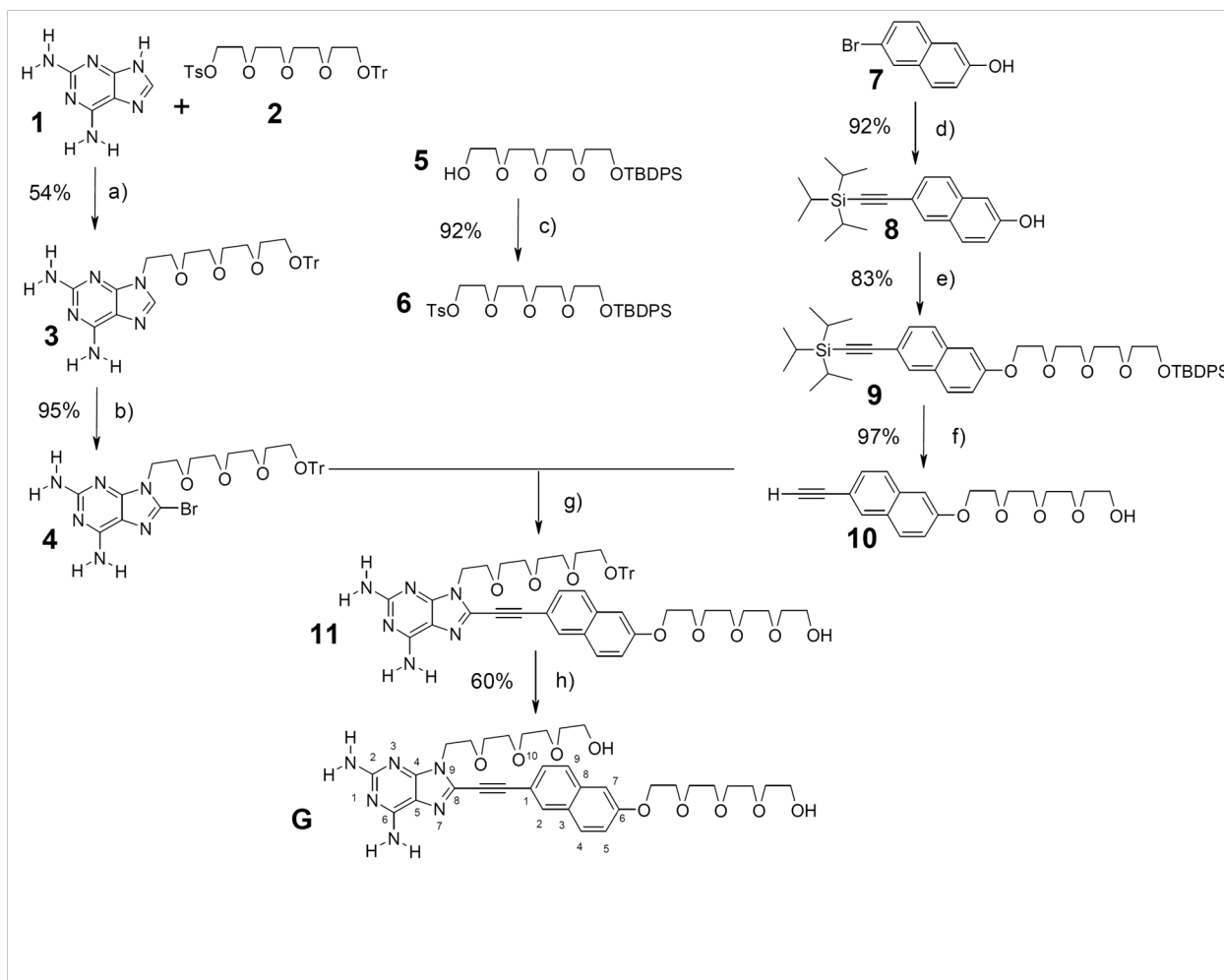


Figure 1: Synthetic route to **G**. a) 1) NaH, DMF, 0°C, 3 hr. 2) **2**, 60°C, 12 hr. b) NBS, MeCN, 1.5 hr. c) 1) NaOH, THF/H<sub>2</sub>O, 0°C, 10 min. 2) TsCl, rt, 3 hr. d) Pd(PPh<sub>3</sub>)<sub>2</sub>Cl<sub>2</sub>, TIPSE, CuI, Et<sub>3</sub>N, 70°C, 12 hr. e) **6**, K<sub>2</sub>CO<sub>3</sub>, DMF, 70°C, 36 hr. f) TBAF, THF, rt, 1 hr. g) Pd(PPh<sub>3</sub>)<sub>4</sub>, piperidine, 70°C, 12 hr. h) TFA, CH<sub>2</sub>Cl<sub>2</sub>, rt, 1 hr.

### 9-Tetraethylene glycol monotrityl-purine-2,6-diamine, **3**

2,6-diaminopurine, **1**, (10 mmol, 1.5 g) was dissolved in DMF (6 ml) and NaH 60% (11 mmol, 0.44 g) was added under argon at 60°C and stirred. After 3 hr, a white solid appeared and trityl tetraethylene glycol *p*-tosyl diether, **2**, (10 mmol, 5.9 g) dissolved in DMF (15 ml) was added at

–5°C. After stirring 12 hr at room temperature, the DMF was evaporated in *vacuo*. Using column chromatography, with CHCl<sub>3</sub>:MeOH (30:1 to 10:1) as the eluent, pure **3** was obtained (2.22 g, 54%). <sup>1</sup>H NMR δ (CDCl<sub>3</sub>, ppm); 3.23 (t, J = 5.1 Hz, 2H, CH<sub>2</sub>OTr), 3.56—3.76 (m, 12H, OCH<sub>2</sub>), 4.16 (t, J = 5.1 Hz, 2H, CH<sub>2</sub>OTs), 4.85 (*s*<sub>broad</sub>, 2H, NH<sub>2</sub>), 5.51 (*s*<sub>broad</sub>, 2H, NH<sub>2</sub>), 7.19—7.31 (m, 9H, ArH<sub>*p*-trityl</sub>, ArH<sub>*m*-trityl</sub>), 7.46 (d, J = 1.5 Hz, 6H, ArH<sub>*o*-trityl</sub>), 7.64 (s, 1H, H<sub>8-purine</sub>). <sup>13</sup>C NMR δ (CDCl<sub>3</sub>, ppm); 43.08 (CH<sub>2</sub>N<sub>Pu</sub>), 63.31 (CH<sub>2</sub>O-Tr), 69.33 (CH<sub>2</sub>-CH<sub>2</sub>-N<sub>Pu</sub>), 70.58, 70.62, 70.67, 70.73, 70.77 (CH<sub>2</sub>O), 86.52 (C<sub>Tr</sub>), 114.18 (C<sub>5-Pu</sub>), 126.91 (C<sub>*p*-Tr</sub>), 127.74 (C<sub>*o*-Tr</sub>), 128.71 (C<sub>*m*-Tr</sub>), 139.28 (C<sub>8-Pu</sub>), 144.11 (C<sub>*ipso*-Tr</sub>), 151.99 (C<sub>4-Pu</sub>), 155.74 (C<sub>6-Pu</sub>), 159.75 (C<sub>2-Pu</sub>). MS (MALDI-TOF); Calc.: 568.28, found: (M + H) = 569.21 g/mol.

### **8-Bromo-9-tetraethylene glycol monotrityl-purine-2,6-diamine, 4**

Purine derivative **3** (1.78 mmol, 1.015 g) was dissolved in CH<sub>3</sub>CN and NBS (1.96 mmol, 0.35 g) was added in small portions during a period of 1.5 hr at room temperature under constant stirring. The solvent was then removed in *vacuo*. Compound **4** was obtained as a pure white solid by column chromatography using CHCl<sub>3</sub>:MeOH (30:1 to 10:1) as the eluent (1.10 g, 95%). <sup>1</sup>H NMR δ (CDCl<sub>3</sub>, ppm); 3.23 (t, J = 5.1 Hz, 2H, CH<sub>2</sub>OTr), 3.60—3.67 (m, 10H, OCH<sub>2</sub>), 3.78 (t, J = 5.9 Hz, 2H, CH<sub>2</sub>CH<sub>2</sub>N<sub>Pu</sub>), 4.21 (t, J = 5.9 Hz, 2H, CH<sub>2</sub>N<sub>Pu</sub>), 4.88 (*s*<sub>broad</sub>, 2H, NH<sub>2</sub>), 5.48 (*s*<sub>broad</sub>, 2H, NH<sub>2</sub>), 7.19—7.30 (m, 9H, ArH<sub>*m*-Tr</sub>, ArH<sub>*p*-Tr</sub>), 7.45 (d, J = 7.3 Hz, 6H, ArH<sub>*o*-Tr</sub>). <sup>13</sup>C NMR δ (CDCl<sub>3</sub>, ppm); 43.46 (CH<sub>2</sub>N<sub>Pu</sub>), 63.29 (CH<sub>2</sub>O-Tr), 68.39 (CH<sub>2</sub>-CH<sub>2</sub>-N<sub>Pu</sub>), 70.61, 70.64, 70.71, 70.76, 70.79 (CH<sub>2</sub>O), 86.52 (C-Tr), 114.46 (C<sub>5-Pu</sub>), 123.89 (C<sub>8-Pu</sub>), 126.90 (C<sub>*p*-Tr</sub>), 127.73 (C<sub>*o*-Tr</sub>), 128.71 (C<sub>*m*-Tr</sub>), 144.12 (C<sub>*ipso*-Tr</sub>), 153.25 (C<sub>4-Pu</sub>), 154.62 (C<sub>6-Pu</sub>), 159.49 (C<sub>2-Pu</sub>). MS (MALDI-TOF); Calc.: 646.19, found: (M + H) = 649.14 g/mol.

### ***tert*-Butyldiphenylsilyl tetraethylene glycol *p*-tosyl diether, 6**

Tetraethylene glycol mono(*tert*-butyldiphenylsilyl) ether, **5**, (16 g, 37 mmol) and NaOH (7.8 g, 200 mmol) were dissolved in 100 ml H<sub>2</sub>O:THF mixture (3:1). At 0°C a THF solution of *p*-tosyl chloride (8.11 g, 42.5 mmol) was added dropwise. After stirring for 3 hr, 50 ml water was added

and the mixture was extracted with diethyl ether. The combined organic layers were washed with water, dried over Na<sub>2</sub>SO<sub>4</sub> and concentrated to obtain **6** as a pure colorless oil (20 g, 92%). <sup>1</sup>H NMR δ (CDCl<sub>3</sub>, ppm); 1.04 (s, 9H, C(CH<sub>3</sub>)<sub>3</sub>), 1.85 (m, 3H, CH<sub>3</sub>-Ts), 3.57—3.79 (t, 12H, OCH<sub>2</sub>), 3.81 (t, TBDPS-OCH<sub>2</sub>), 4.14 (t, Ts-OCH<sub>2</sub>), 7.32 (d, J = 8.0 Hz, 2H, TsH<sub>m</sub>), 7.39 (m, 6H, TBDPSH<sub>m,p</sub>), 7.68 (dd, J<sub>1</sub> = 1.6 Hz, J<sub>2</sub> = 5.6 Hz, TBDPSH<sub>o</sub>), 7.79 (d, J = 8.0 Hz, TsH<sub>o</sub>). <sup>13</sup>C NMR δ (CDCl<sub>3</sub>, ppm): 19.18 (C(CH<sub>3</sub>)<sub>3</sub>), 21.62 (CH<sub>3</sub>Ts), 26.81 (C(CH<sub>3</sub>)<sub>3</sub>), 63.41, 68.67, 68.21, 70.71, 72.43 (CO), 127.61 (C<sub>m-TBDPS</sub>, C<sub>o-Ts</sub>), 127.97 (C<sub>m-Ts</sub>), 129.60 (C<sub>p-TBDPS</sub>), 129.79 (CSi), 133.69 (CS), 135.60 (C<sub>o-TBDPPUS</sub>).

### **6-[Triisopropylsilylethynyl]-2-naphthol, 8**

A Schlenk tube was charged with Et<sub>3</sub>N (5 ml), 6-bromo-2-naphthol (2.69 g, 11.2 mmol) and triisopropylsilylethyne (4.4 g, 22.4 mmol) and deoxygenated by purging argon through the mixture. Subsequently Pd(PPh<sub>2</sub>)<sub>2</sub> (0.63 g, 0.9 mmol) and 42 mg of CuI were added. The reaction mixture was stirred 12 hr at 70°C. After removal of the volatiles and column chromatography with CHCl<sub>3</sub> as the eluent (3.1 g, 92%), compound **8** was obtained as a brown wax. <sup>1</sup>H NMR δ (CDCl<sub>3</sub>, ppm); 1.15 (m, 21H, CH<sub>3</sub> and CH), 5.05 (*s<sub>broad</sub>*, 1H, OH), 7.09 (d, J = 2.8 Hz, 1H, NaH<sub>3Na</sub>), 7.11 (s, 1H, NaH<sub>1Na</sub>), 7.48 (dd, J<sub>1</sub> = 1.6 Hz, J<sub>2</sub> = 8.0 Hz, 1H, NaH<sub>8Na</sub>), 7.59 (d, J = 8.8 Hz, 1H, NaH<sub>7Na</sub>), 7.69 (dd, J<sub>1</sub> = 1.6 Hz, J<sub>2</sub> = 8.0 Hz, 1H, NaH<sub>4Na</sub>), 7.92 (s, 1H, NaH<sub>5Na</sub>).

### **6-[Triisopropylsilylethynyl]-2-naphthol [*tert*-butyldiphenylsilyl tetraethylene glycol] ether, 9**

Naphthol **8** (2.35 g, 7.24 mmol), tosylate **6** (4.67 g, 7.97 mmol) and K<sub>2</sub>CO<sub>3</sub> (3 g) were stirred in 30 ml DMF at 70°C. After 36 hr water was added and the mixture was extracted with isopropyl ether, dried with MgSO<sub>4</sub> and concentrated. Column chromatography with isopropyl ether as the eluent afforded **9** as a yellow oil (4.45 g, 83%). <sup>1</sup>H NMR δ (CDCl<sub>3</sub>, ppm); 1.04 (s, 9H, C(CH<sub>3</sub>)<sub>3</sub>), 1.16 (m, 21H, CH<sub>3</sub> and CH), 3.59—3.82 (t, 12H, OCH<sub>2</sub>), 3.91 (t, 2H, SiOCH<sub>2</sub>), 4.23 (t, 2H,

NaOCH<sub>2</sub>), 7.08 (s, 1H, NaH<sub>1Na</sub>), 7.16 (dd, J<sub>1</sub> = 1.6 Hz, J<sub>2</sub> = 8.0 Hz, 1H, NaH<sub>3Na</sub>), 7.37 (m, 6H, TBDPSH<sub>m,p</sub>), 7.47 (d, J = 8.0 Hz, 1H, NaH<sub>8Na</sub>), 7.62 (d, J = 8.0 Hz, 1H, NaH<sub>7Na</sub>), 7.66 (d, J = 8.0 Hz, 1H, NaH<sub>4Na</sub>), 7.69 (dd, J<sub>1</sub> = 1.6 Hz, J<sub>2</sub> = 5.6 Hz, TBDPSH<sub>o</sub>), 7.91 (s, 1H, NaH<sub>5Na</sub>).

### **6-Ethynyl-2-naphthol tetraethylene glycol ether, 10**

A mixture of naphthalene derivative **9** (4 g, 5.41 mmol) and 13.5 ml of a 1 M TBAF solution in THF were stirred for 1 hr. Column chromatography using CH<sub>2</sub>Cl<sub>2</sub>:MeOH (99:1 to 94:6) as the eluent yielded **10** as a pure white solid (1.95 g, 97%). <sup>1</sup>H NMR δ (CDCl<sub>3</sub>, ppm): 2.52 (*s<sub>broad</sub>*, 1H, OH), 3.10 (s, C≡CH), 3.59—3.77 (t, 12H, OCH<sub>2</sub>), 3.92 (t, CH<sub>2</sub>OH), 4.26 (t, 2H, NaOCH<sub>2</sub>), 7.11 (d, J = 1.6 Hz, NaH<sub>1Na</sub>), 7.19 (dd, J<sub>1</sub> = 1.6 Hz, J<sub>2</sub> = 8.0 Hz, 1H, NaH<sub>3Na</sub>), 7.48 (dd, J<sub>1</sub> = 1.6 Hz, J<sub>2</sub> = 8.0 Hz, 1H, NaH<sub>7Na</sub>), 7.65 (d, J = 8.0 Hz, 1H, NaH<sub>8Na</sub>), 7.69 (d, J = 8.0 Hz, NaH<sub>4Na</sub>), 7.94 (s, 1H, NaH<sub>5Na</sub>).

### **8-[2-Tetraethylene glycol-6-ethynyl-naphthalene]-9-tetraethylene glycol-purine-2,6-diamine, G**

The brominated purine **4** (0.9 mmol, 0.50 g) and the naphthalene derivative **9** (0.9 mmol, 0.31 g) were dissolved in deoxygenated piperidine (15 ml). Subsequently, the catalyst Pd(PPh<sub>3</sub>)<sub>4</sub> (0.029 mmol, 0.033 g) was added and the flask was sealed and stirred overnight at 70°C, prior to removal of piperidine in *vacuo*. The intermediate **11** was obtained after column chromatography using CHCl<sub>3</sub>:MeOH (30:1) as the eluent. Intermediate **11** was deprotected in 1 hr in a TFA/THF mixture (10% in 5 ml THF) at room temperature. Title compound **G** was obtained pure as a brownish solid after column chromatography using CHCl<sub>3</sub>:MeOH (30:1) as the eluent (0.350 g, 60%). <sup>1</sup>H NMR δ (CDCl<sub>3</sub>, ppm); 3.46—3.78 (m, 24H, OCH<sub>2</sub>), 3.87 (t, J = 5.87 Hz, 2H, OCH<sub>2</sub>CH<sub>2</sub>Npu), 3.93 (t, J = 4.76 Hz, 2H, OCH<sub>2</sub>CH<sub>2</sub>ONa), 4.28 (t, J = 4.6 Hz, 2H, CH<sub>2</sub>Npu), 4.33 (t, J = 5.7 Hz, 2H, CH<sub>2</sub>ONa), 5.08 (*s<sub>broad</sub>*, 2H, NH<sub>2</sub>), 5.77 (*s<sub>broad</sub>*, 2H, NH<sub>2</sub>), 7.09 (s, 1H, NaH<sub>1Na</sub>), 7.18 (dd, J<sub>1</sub> = 2.4 Hz and J<sub>2</sub> = 9.2 Hz, 1H, NaH<sub>3Na</sub>), 7.50 (dd, J<sub>1</sub> = 2.2 Hz, J<sub>2</sub> = 8.6 Hz, 1H, NaH<sub>7Na</sub>), 7.63 (d, J

= 8.4 Hz, 1H, NaH<sub>8Na</sub>), 7.65 (d, J = 9.2 Hz, NaH<sub>4Na</sub>), 7.97 (s, 1H, NaH<sub>5Na</sub>). <sup>13</sup>C NMR δ (CDCl<sub>3</sub>, ppm); 45.78 (CH<sub>2</sub>-N<sub>Pu</sub>), 61.57, 61.52 (CH<sub>2</sub>-OH), 67.52 (CH<sub>2</sub>-O<sub>Na</sub>), 68.72 (CH<sub>2</sub>-CH<sub>2</sub>-N<sub>Pu</sub>), 69.64 (CH<sub>2</sub>-CH<sub>2</sub>-O<sub>Na</sub>), 70.27, 70.34, 70.46, 70.56, 70.59, 70.69, 70.80, 70.83 (CH<sub>2</sub>-O), 72.63, 72.71 (CH<sub>2</sub>-CH<sub>2</sub>-OH), 81.04, 84.48 (C≡C), 106.82 (C<sub>7Na</sub>), 113.89, 113.91 (C<sub>9Na</sub>, C<sub>1Na</sub>), 115.81 (C<sub>5-Pu</sub>), 120.04 (C<sub>8-Pu</sub>), 127.12, 128.43, 129.50, 132.12 (C<sub>2Na</sub>, C<sub>5Na</sub>, C<sub>6Na</sub>, C<sub>10Na</sub>), 133.11, 134.68 (C<sub>3Na</sub>, C<sub>4Na</sub>), 151.80 (C<sub>4-Pu</sub>), 153.19 (C<sub>8Na</sub>), 154.35 (C<sub>6-Pu</sub>), 158.02 (C<sub>2-Pu</sub>). MS (MALDI-TOF); Calc.: 668.32, found: (M + H) = 669.28 g/mol.

## Subtraction of excess donor background

In order to extract from the TCSPC data the NP excitation decay arising *solely* from energy transfer to the acceptor, we first corrected the data for the background arising from excess NP added in order to promote filling of all available template sites. For each available base of the DNA template, four NP molecules were available, i.e. an excess of three per binding site. At low temperatures  $T$  (e.g. 15°C), the PL decay from the donor can thus be described by

$$I_D^{15^\circ\text{C}} = \hat{I}_D \left[ \eta_{\text{bound}} N_{\text{bound}}^{15^\circ\text{C}} \exp\left(-\frac{t}{\tau_{D,\text{bound}}}\right) + \eta_{\text{free}} N_{\text{free}}^{15^\circ\text{C}} \exp\left(-\frac{t}{\tau_{D,\text{free}}}\right) \right]. \quad (1)$$

Here  $\tau_{D,\text{bound}}$  and  $\tau_{D,\text{free}}$  are the lifetimes of excitations on NP bound to the template, and those on excess, unbound NP, respectively,  $N_{\text{bound}}^{15^\circ\text{C}}$  and  $N_{\text{free}}^{15^\circ\text{C}}$  are the numbers of free and bound NP donors excited in the imaged volume of solution (at 15°C), and  $\eta_{\text{bound}}$  and  $\eta_{\text{free}}$  the quantum efficiencies of emission of the free and bound NP, respectively. At elevated temperatures (e.g. 50°C), all NP are detached from the templates, and the donor PL decay is given by

$$I_D^{50^\circ\text{C}} = \hat{I}_D \eta_{\text{free}} N_{\text{free}}^{50^\circ\text{C}} \exp\left(-\frac{t}{\tau_{D,\text{free}}}\right). \quad (2)$$

For the complex, energy transfer at a rate  $k_{ET}(t)$  has to be considered as an additional de-excitation pathway for NP, and the PL decay at low temperatures can be described by

$$I_C^{15^\circ C} = \hat{I}_C \left[ \eta_{bound} N_{bound}^{15^\circ C} \exp\left(-\frac{t}{\tau_{D,bound}} - k_{ET} t\right) + \eta_{free} N_{free}^{15^\circ C} \exp\left(-\frac{t}{\tau_{D,free}}\right) \right], \quad (3)$$

At high temperatures, again all NP are detached from the template which leads to the suppression of energy transfer and all luminescence originates from unbound NP, i.e.

$$I_C^{50^\circ C} = \hat{I}_C \eta_{free} N_{free}^{50^\circ C} \exp\left(-\frac{t}{\tau_{D,free}}\right). \quad (4)$$

Using Equations 1 to 4, the energy transfer dynamics  $I_{ET}$  can now be extracted by calculating first the PL decay components associated only with NP *bound to the templates*, as

$$X \equiv I_D^{15^\circ C} - \frac{N_{free}^{15^\circ C}}{N_{free}^{50^\circ C}} I_D^{50^\circ C} = \hat{I}_D \exp\left(-\frac{t}{\tau_{D,bound}}\right) \quad (5)$$

and

$$Y \equiv I_C^{15^\circ C} - \frac{N_{free}^{15^\circ C}}{N_{free}^{50^\circ C}} I_C^{50^\circ C} = \hat{I}_C \exp\left(-\frac{t}{\tau_{D,bound}} - k_{ET} t\right). \quad (6)$$

From Eqns. 5 and 6 the energy transfer dynamics can then be determined through

$$I_{ET} = \frac{Y}{X} = \hat{I}_{ET} e^{(-k_{ET} t)}, \quad (7)$$

provided that the fraction  $f = \frac{N_{free}^{15^\circ C}}{N_{free}^{50^\circ C}}$  is known. In general  $f$  can be directly calculated from the absorption coefficients  $\alpha_{15^\circ C}$  and  $\alpha_{50^\circ C}$  of the cold and hot solutions. However, for the experiments presented here, the absorption coefficients were small compared to the length of the imaged volume and the two absorption coefficients were very similar at the excitation wavelength used. For these cases,  $f$  is simply given by the concentration ratio

$$f = \frac{c_{free}}{c_{free} + c_{bound}} \quad (8)$$



i.e. it is the fraction  $f=0.75$  of NP molecules that are free (unbound) even at low ( $15^{\circ}\text{C}$ ) temperature as a result of the addition of excess NP.

In determining  $I_{ET}$  in this manner, we assumed that at temperatures of  $50^{\circ}\text{C}$  and over, all NP molecules present in the samples are not hydrogen-bonded to the template. TCSPC delay traces confirmed this assumption: the non-normalized intensities of the donor samples for arbitrary oligothymine length (at a detection wavelength of 507 nm) converged to a baseline PL decay that did not change significantly between  $50^{\circ}\text{C}$  and  $70^{\circ}\text{C}$ . Another indication that the assemblies have fragmented at  $50^{\circ}\text{C}$  is the flattening of the temperature-dependence of  $\tau_D$  values at this temperature (see Figure 3(b) of the main paper). For a given low temperature  $T$  (e.g. for  $15^{\circ}\text{C}$  as described above), the transfer dynamics were thus calculated using Equations 1 to 7 with  $50^{\circ}\text{C}$  as the high-temperature reference point for which all NP are assumed to be free. Figure 2 illustrates the results of such calculations for  $T=15^{\circ}\text{C}$ .

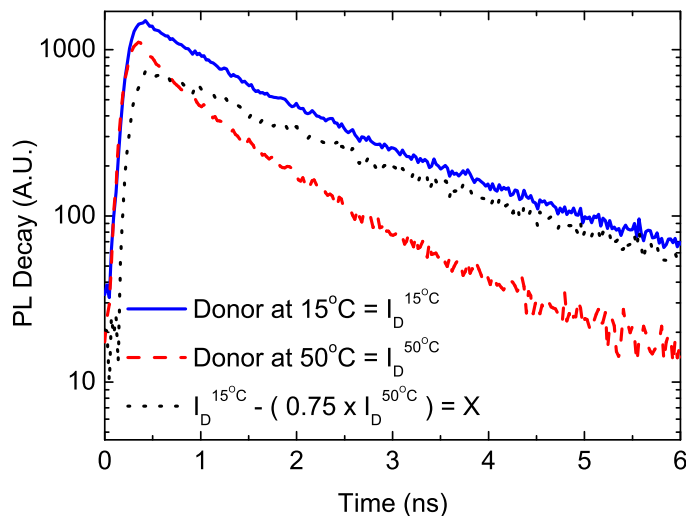


Figure 2: Photoluminescence (PL) decays illustrating the procedure involved in removing the excess NP contribution from the assembled NP photoluminescence decay contribution.  $I_D^{15^{\circ}\text{C}}$  is the PL decay of a  $n$ -base oligothymine-NP assembly at a low temperature ( $15^{\circ}\text{C}$ , for example), where  $n$  is the number of thymines.  $I_D^{50^{\circ}\text{C}}$  is the PL decay of a  $n$ -base oligothymine-NP assembly at a high enough temperature at which all NP are assumed not to be bonded to the oligothymine.  $X$  is the NP-excess corrected decay solely from excitations on NP hydrogen-bonded to the template.

## Further details on modeling of energy transfer dynamics

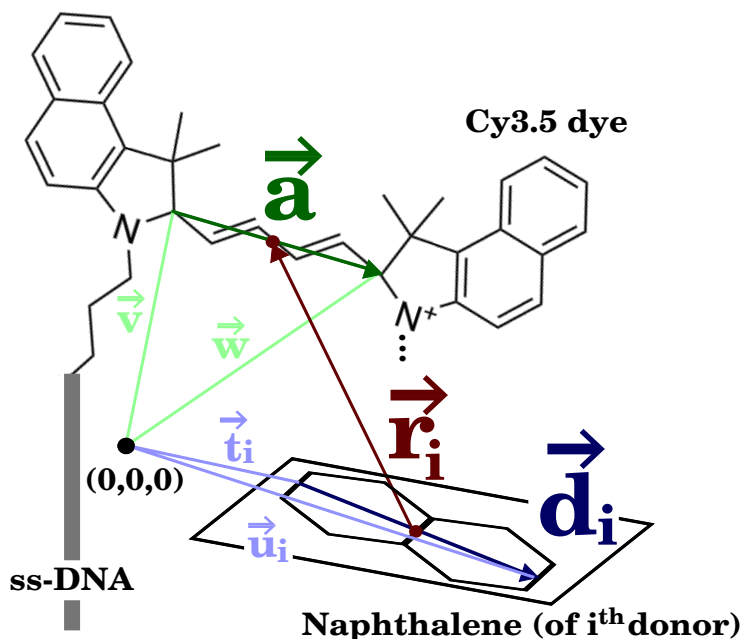


Figure 3: Schematic of the donor-acceptor complex structure consisting of a Cy3.5 dye covalently bonded to the end of a strand of 40 thymine bases. 40 naphthalene chromophore donors are arranged at intervals along the length of the strand. The acceptor absorption transition dipole across the polymethyne bridge is represented by  $\vec{a}$ ; the  $i^{\text{th}}$  donor emission transition dipole across the long axis of the  $i^{\text{th}}$  naphthalene, by  $\vec{d}_i$ ; the distance from the center of the acceptor dipole to the center of the  $i^{\text{th}}$  donor dipole  $\vec{r}_i$ , which was extracted from the shown atomic positions using  $\vec{r}_i = \frac{1}{2} [\vec{w} + \vec{v} - (\vec{t}_i + \vec{u}_i)]$ .

For modelling of the energy transfer dynamics the real geometric assembly geometry of the complexes was taken into account when donor-acceptor distances  $r_i$  and orientation factors  $\kappa_i$  were calculated for each donor-acceptor pair. For this purpose, the vectors representing each donor dipole moment direction,  $\vec{d}_i$ , the acceptor dipole moment,  $\vec{a}$ , and that connecting the centers of these moments,  $\vec{r}_i$ , were determined using atom positions, relative to a common origin, in the geometry-optimized 40-donor complex from molecular simulations. Figure 3 illustrates how these vectors were extracted for a particular  $i$ -th base donor and acceptor combination. For the calculations of the energy transfer dynamics as described in the main text,  $r_i$  and  $\kappa_i$  were determined from these

Table 1: Separations  $r_i$  between the center of the dipole on the acceptor chromophore and the center of the dipole on the naphthalene of the  $i^{th}$  donor molecule, as shown in Figure 3.  $\kappa_i^2$ , which was calculated with Eqn. 9, defines the orientation dependence of the acceptor and donor dipoles on the Förster radius as described in the main text.

$i$	$r_i$ (nm)	$\kappa_i^2$	$i$	$r_i$ (nm)	$\kappa_i^2$
1	1.95	2.40685	21	7.21	0.28361
2	1.98	1.28356	22	7.42	0.00002
3	1.69	0.50905	23	7.63	0.20985
4	1.58	0.62685	24	7.78	0.98464
5	1.60	0.73086	25	8.10	1.19226
6	1.80	0.29898	26	8.40	0.47828
7	1.99	0.06079	27	8.74	0.00006
8	2.42	0.26614	28	9.09	0.22375
9	3.65	0.09963	29	10.00	0.96288
10	3.80	0.28050	30	10.32	0.72603
11	3.92	0.11810	31	10.46	0.31253
12	4.39	0.00050	32	10.62	0.00043
13	4.55	0.18688	33	11.02	0.07953
14	4.54	0.47728	34	11.41	0.97169
15	4.80	0.90628	35	11.44	0.75733
16	5.20	0.18459	36	11.91	0.05555
17	5.44	0.08336	37	12.27	0.00219
18	6.44	0.10414	38	12.78	0.66885
19	6.72	0.88967	39	13.17	1.03577
20	6.92	0.95725	40	13.33	0.73948

vectors using

$$\kappa_i^2 = \left[ \frac{\vec{a} \cdot \vec{d}_i}{\|\vec{a}\| \|\vec{d}_i\|} - 3 \frac{(\vec{d}_i \cdot \vec{r}_i)(\vec{a} \cdot \vec{r}_i)}{\|\vec{d}_i\| \|\vec{a}\| \|\vec{r}_i\|^2} \right]^2 \quad \text{and} \quad r_i = \|\vec{r}_i\| \quad (9)$$

where  $\|\vec{a}\|$  is the norm or length of a vector  $\vec{a}$ .

Table 1 lists the values of  $r_i$  and  $\kappa_i$  obtained in this manner for the modelled assembly containing  $n=40$  bases. It is interesting to note that for the realistic simulated structure examined here, the first NP of the template is not necessarily the closest to the Cy3.5 acceptor dye. Furthermore, full Molecular Dynamics simulation of the 10-base system on the 10 ns timescale reveals the structure globally collapses, i.e. the diaminopurines of the donors do not strictly remain H-bonded in Watson-Crick arrangement because of the base-flipping, naphthalene reorientation, and coiling of the ethylene oxide groups.

The quantum efficiency of the bound donors,  $\eta_D$ , used in the calculations was determined using  $\eta_{15^\circ\text{C}} = 0.25\eta_D + 0.75\eta_{50^\circ\text{C}}$  in representation of the relative presences of bound and free donors in solution at low temperature, where  $\eta_{15^\circ\text{C}}$  is the quantum efficiency measured for the solutions at  $15^\circ\text{C}$  and  $\eta_{50^\circ\text{C}}$  that measured at  $50^\circ\text{C}$ , yielding  $\eta_D=0.9$ .

## References

- (1) A. Altomare, F. Ciardelli, B. Gallot, M. Mader, R. Solaro, N. Tirelli, J. Polym. Sci. Part A: Polym. Chem. (2001) p. 2957.
- (2) C. W. Dicus, M. H. Nantz, Synlett (2006) p. 2821.
- (3) a) T.C. Norman, N.S. Gray, J.T. Koh, P. Schultz, J. Am. Chem. Soc. (1996) p. 7430; b) A. Hol, J. Gnter, H. Dvokov, M. Masojdkov, G. Andrei, R. Snoeck, J. Balzarini, E. De Clercq, J. Med. Chem. (1999) p. 2064.
- (4) R. Chinchilla, C. Najera, Chem. Rev. (2007) p. 874.
- (5) T. H. Förster, Discuss. Faraday Soc. (1959) p. 7.
- (6) L. M. Herz, C. Silva, A. C. Grimsdale, K. Müllen, and R. T. Phillips, Phys. Rev. B (2004) p. 165207.
- (7) P. Parkinson, E. Aharon, M. H. Chang, C. Dosche, G. L. Frey, A. Köhler, and L. M. Herz, Phys. Rev. B (2007) p. 165206.